

# Interaction forces between DPPC bilayers on glass

*Raquel Orozco-Alcaraz and Tonya L. Kuhl\**

University of California Davis. Department of Chemical Engineering and Materials Science, One Shields Avenue, Davis CA 95616

\*E-mail: [tkuhl@ucdavis.edu](mailto:tkuhl@ucdavis.edu)

**Supporting Information Part 1: Experimental comparison between multilayer matrix model and the 3-layer and 5-layer multiple beam interferometry models. Fluorescent microscopy images of supported DPPC membranes on mica and silica coated mica.**

The primary objective in surface force apparatus (SFA) interferometry measurements is to determine the distance (or separation) between the substrates. The distance is determined from the wavelength positions of the fringes of equal chromatic order (FECO) formed from the constructive interference of light passing through the surfaces. The interferometry data from the surface force apparatus (SFA) is analyzed by solving the optical equations using a multilayer matrix model (MMM) or analytical solutions based on multiple beam interferometry (MBI). MMM, described previously<sup>1-4</sup>, is derived from Maxwell's equations and can be used to numerically calculate the FECO wavelengths obtained from an optical interferometer if the thickness and refractive index (RI) of each layer in the interferometer are known<sup>2,4</sup>. Analytical expressions based on MBI exist for 3 and 5-layer symmetrical interferometers.<sup>5</sup> Note that in MBI the silver layers are not accounted for in the calculations whereas in MMM all layers are taken into consideration. Thus every time we describe the number of layers in MMM, the silver layers are included. This means that for the same interferometer in MMM notation has two extra layers

than MBI notation. For asymmetric systems or when more than 7 layers are involved MMM is employed.

Our experiments are based on the interaction between lipid bilayers deposited on SiO<sub>2</sub>-coated mica back silvered surfaces in water. This system requires a MMM solution of a 9-layer interferometer. In this supplement we describe our in-house MMM algorithm and the steps we take to establish the thickness and refractive index for each layer in the interferometer. Finally, we demonstrate that the analytical 5-layer MBI solution is a very good approximation to the more complicated MMM approach for obtaining surface separation or gap thickness.

We have developed both Mathematica and MatLab MMM algorithms to fit the thickness and refractive index from each layer in the optical interferometer. The algorithm closely follows what was proposed by Clarkson<sup>2</sup> and Mangipudi<sup>4</sup>. The program essentially matches the wavelength peaks of FECO measurements with the appropriate layer thickness and refractive index for each layer. The following are the program inputs and approach:

1. Wavelength peaks of FECO obtained from a spectrometer coupled to the SFA.
2. Wavelength peaks from the Hg spectrum (green and yellow lines), which are used as a calibration tool.
3. Estimated or known thickness (minimum, maximum) for each layer. The initial value for the SiO<sub>2</sub> layer is based on thickness measurements during the e-beam deposition from the quartz crystal resonator. The mica thickness is based on control measurements for the same thickness of mica without the SiO<sub>2</sub> layer.
4. Estimated or known refractive index (RI) (minimum, maximum) for each layer. For example the known refractive index of silver ( $n=0.05$ ) is used. However, mica is a natural mineral whose refractive index can vary slightly between samples and is thus fit.

5. Because of the large number of fitting parameters, the phase space is restricted by maximum and minimum values based on known physical parameters. The smallest sum of square error (SSE) between the measured FECO wavelengths and the MMM calculated FECO wavelengths is chosen to obtain thicknesses and RI of the various layers. In all cases, the SSE was  $\ll 1$ .

To observe and measure the FECO wavelengths, we utilized a SpectraPro-3/4 meter spectrometer with an integrated Princeton SPEC-10:2K Digital CCD camera. Figure S1 shows an example CCD image for 1028Å thick SiO<sub>2</sub> on 4.4µm thick mica. Figure S2 illustrates the intensity spectrum as a function of wavelength for a FECO image. Peak wavelength positions are obtained with Igor Pro using the Multi-peak Fitting analysis package.

### Analysis procedure:

For completeness, we have included the MMM equations taken directly from literature and programmed in our in-house algorithm. The characteristic matrix for an interferometer consisting of L layers can be written as:

$$\bar{M} = \prod_j^L \bar{M}_j = \begin{bmatrix} m_{11} & m_{12} \\ m_{21} & m_{22} \end{bmatrix} \quad (1)$$

Where characteristic matrix for each layer, j, is:

$$\bar{M}_j = \begin{bmatrix} \cos\left(\frac{2\pi\bar{u}_j D_j \cos\theta_j}{\lambda}\right) & -\left(\frac{i}{\bar{u}_j \sqrt{\epsilon_0}}\right) \sin\left(\frac{2\pi\bar{u}_j D_j \cos\theta_j}{\lambda}\right) \\ -i\bar{u}_j \sqrt{\epsilon_0} \sin\left(\frac{2\pi\bar{u}_j D_j \cos\theta_j}{\lambda}\right) & \cos\left(\frac{2\pi\bar{u}_j D_j \cos\theta_j}{\lambda}\right) \end{bmatrix} \quad (2)$$

the transmission coefficient is expressed as:

$$t = \frac{2\bar{u}_0 \sqrt{\epsilon_0}}{(m_{11} + m_{12} \bar{u}_0 \sqrt{\epsilon_0}) \bar{u}_0 \sqrt{\epsilon_0} + m_{21} + m_{22} \bar{u}_0 \sqrt{\epsilon_0}} \quad (3)$$

and the transmittivity is:

$$T = t \times t^* \quad (4)$$

Here  $D_j$  and  $\bar{u}_j$  are the thickness and the complex refractive index of layer  $j$ , respectively.  $\bar{u}_0$  is the refractive index of the medium surrounding the interferometer,  $\theta_j$  is the angle of incidence on layer  $j$ ,  $\epsilon_0$  is the permittivity of space,  $\lambda$  is the wavelength of incoming light. If thickness,  $D_j$ , and refractive index,  $u_j$ , for each layer are known, the intensity of the transmitted light can be calculated at a given wavelength. The wavelengths at maximum transmittivity correspond to the wavelengths for each FECO.

The following are the detailed steps taken to obtain Ag, Mica, SiO<sub>2</sub> and bilayer thickness and refractive index for a given experiment. First, the simplest case of Silver-Mica-Silver is used to determine the mica and silver thickness and refractive index of mica. Thermal evaporation is used to deposit silver on a clean piece of mica, and the thickness of the deposited film from the quartz resonator is used as a first guess of the silver thickness (e.g. 550±50Å). The value for the refractive index of silver over the visible spectrum is,  $\eta_{\text{Ag}}=0.05$ .<sup>6</sup> The wavelength spacing of the FECO is used to provide an estimate of the mica thickness. The mica used in these experiments is ruby muscovite which provides an initial guess of refractive index  $\eta_{\text{mica}}=1.58$ . The silver and mica thickness and refractive index of mica are obtained based on the smallest SSE in fitting the experimentally measured FECO positions simultaneously using a 3-layer MMM.

After determining the layer parameters for mica and silver, the thickness and refractive index of SiO<sub>2</sub> is determined utilizing a 5-layer MMM: Ag-Mica-SiO<sub>2</sub>-Mica-Ag, as shown in Figure S3. As described in Materials and Methods section, SiO<sub>2</sub> is deposited uniformly<sup>7</sup> on mica via e-beam deposition. At this point, the only unknowns are the SiO<sub>2</sub>'s refractive index and thickness.

### MBI analytical solution of the 3-layer and 5-layer interferometers

3-layer interferometer: consider the case where a transparent film of thickness  $T$  and refractive index  $u_2$  is sandwiched between two symmetrical films of thickness  $D_1$  and refractive index  $u_1$ , see Figure S3 for illustration. The analytical solution to obtain the gap thickness,  $T$  or  $2D_2$ , between the symmetrical films is the following<sup>5</sup>:

$$\tan(ku_2T) = \frac{2\bar{u} \sin\left(\frac{n\pi\Delta\lambda_n}{\lambda}\right)}{(1+\bar{u}^2) \cos\left(\frac{n\pi\Delta\lambda_n}{\lambda}\right) \pm (\bar{u}^2-1)} \quad (5)$$

Where  $\bar{u} = u_1/u_2$ ,  $n$  is the order of interference or fringe order of the  $n$ th fringe,  $k = 2\pi/\lambda$ , and  $\Delta\lambda_n = \lambda_n - \lambda_n^0$ . The reference wavelength,  $\lambda_n^0$ , is obtained from the position of the  $n^{\text{th}}$  fringe when  $T = 0$ . With this method, the only unknowns are the thickness,  $T$ , and refractive index  $\mu_2$ .

5-layer interferometer: consider the interferometer depicted in Figure S4, where the SiO<sub>2</sub> films are now separated by a water film of thickness  $T$  and refractive index  $\mu_3$ . The general solution for a 5-layer symmetrical interferometer is the following<sup>5</sup>:

$$\begin{aligned} & \tan(ku_3T) \\ &= \frac{(1-r_1^2)\{\sin 2k(u_2D_2+u_1D_1)-2r_2 \sin(2ku_2D_2)+r_2^2 \sin 2k(u_2D_2-u_1D_1)\}}{2r_1\{1-2r_2 \cos(2ku_1D_1)+r_2^2\}-(1+r_1^2)\{\cos 2k(u_2D_2+u_1D_1)-2r_2 \cos(2ku_2D_2)+r_2^2 \cos 2k(u_2D_2-u_1D_1)\}} \end{aligned} \quad (6)$$

Where  $r_1=(u_2-u_3)/(u_2+u_3)$  and  $r_2=(u_1-u_2)/(u_1+u_2)$ . To find the water gap thickness in this case, all other parameters should be known. The refractive indexes should be established and  $D_1$  and  $D_2$  must be determined separately before  $T$  can be obtained, namely when  $T=0$ .

### SiO<sub>2</sub> layer properties

In the original work on e-beam deposited SiO<sub>2</sub> films on mica, Vigil et al.<sup>7</sup> found that the SiO<sub>2</sub> films swell with humidity and reach a maximum and constant thickness in water. The

change in thickness was reported to be  $\sim 20\text{\AA}$ , in agreement with our experiments, see Table S1 for experimental results.

The uniformity of the  $\text{SiO}_2$  thickness and RI underwater was determined by measuring contact between the films in water at various locations. Table S2 lists the thickness, RI, and SSE values obtained using MMM for multiple experiments. In all cases, the minimum SSE was obtained with a refractive index of 1.46 for the  $\text{SiO}_2$  film in agreement with ellipsometer measurements and other literature values<sup>7</sup>.

### **Comparison between 7-layer MMM and analytical solutions of MBI**

One of the most significant differences between MMM and the analytical MBI methods is that MBI provides a simpler and more efficient way to analyze data. The analytical 5-layer solution is comparable with the 7-layer MMM, thus we are interested in determining the error in approximating a 7-layer MMM with a 5-layer and 3-layer MBI solution.

Consider the case where a water layer is in between  $\text{SiO}_2$ -covered mica surfaces and the system is symmetrical, see Figure S4 for illustration. To compute the water gap thickness (T), all other parameters in equations (5) and (6) must be established. To utilize the analytical 3-layer MBI solution for a 5-layer interferometer, we decided to combine the mica and  $\text{SiO}_2$  layers into one with a joint thickness and refractive index. In Table S3, we tabulate the calculated water thickness at different separations for all methods of analysis. We also included the % difference between MMM and MBI.

As shown, the 3-layer MBI provides a good starting estimate for the separation distance for the MMM analysis. Although the  $\text{SiO}_2$  thickness is relatively small compared to the base mica substrates ( $\sim 2\%$  of mica thickness), it has a significant impact in the calculated separation

distance when the system is approximated using only a 3-layer model. The 5-layer model, on the other hand is in very good agreement with MMM.

### **Supporting Information Part 2: Fluorescent images of DPPC bilayers on mica and silica-coated mica**

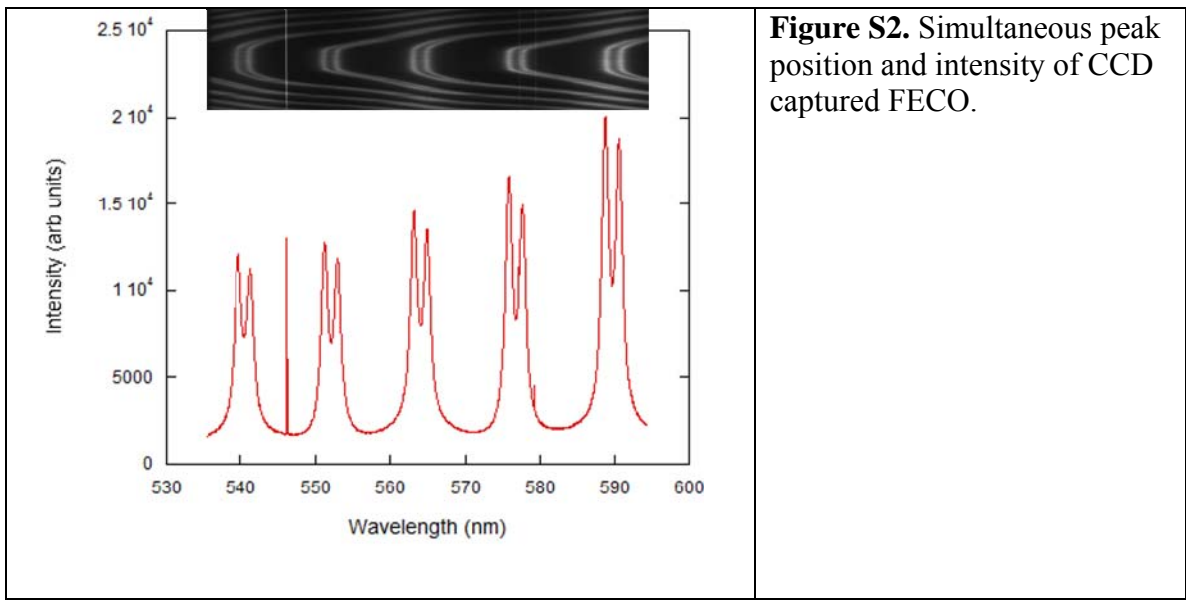
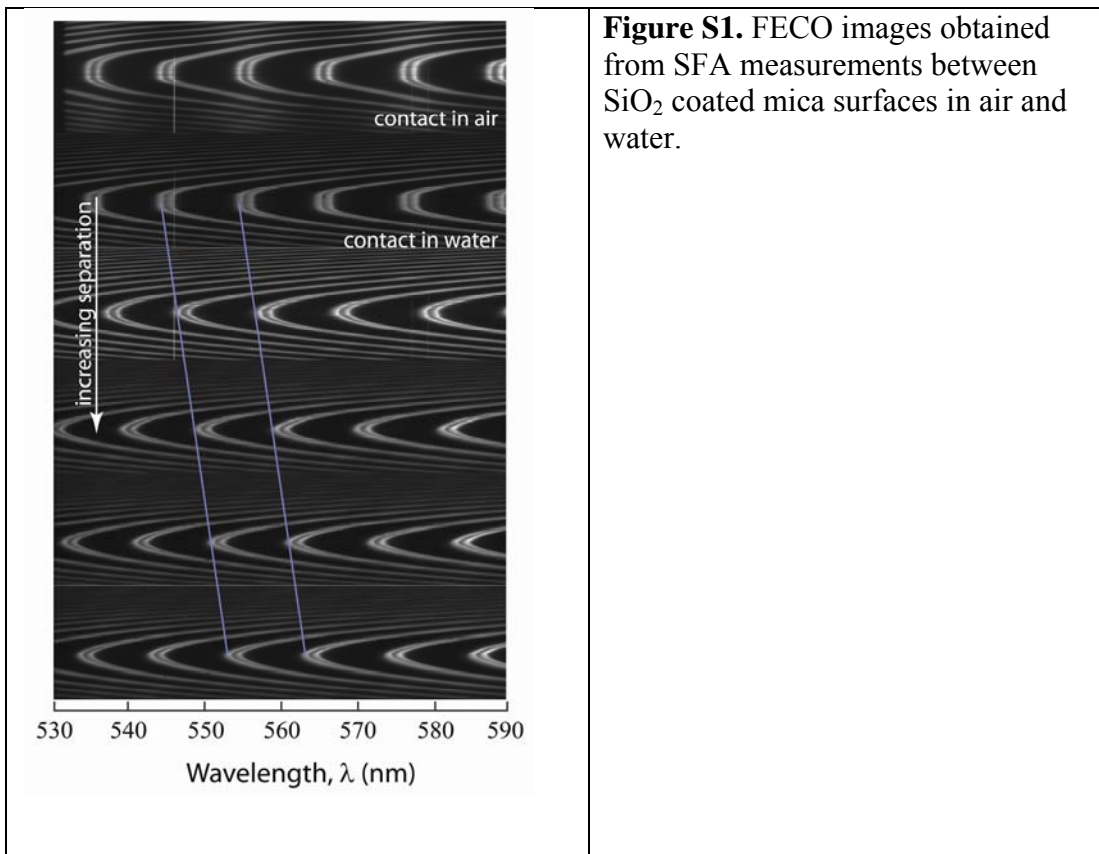
Figure S5 shows representative fluorescent images of LB deposited DPPC bilayers on mica and silica-coated mica containing 1 mole% Texas Red DHPE. The membranes are uniform and very similar in both cases. Small domains appear throughout the images; the uniformity confirms that a well packed membrane exists on both substrates but the resolution of the images does not allow differentiating between the two. Fluorescence recovery after photobleaching (FRAP) measurements were performed to confirm the gel phase state of the DPPC membrane at room temperature. FRAP has been used extensively to measure the lateral diffusion coefficient of model membranes<sup>8-10</sup>. A small area was photobleached with high power light, leaving behind a dark circular region (as seen in Figure S5A and S5B). When the bilayer is in the fluid phase, diffusion drives the lipid components, along with the integrated fluorophore, into/out-of the bleached area leading to a recovery of the bleached spot. No recovery over an hour time scale was observed (Figure S5A and S5B), which is expected for DPPC at 25°C.

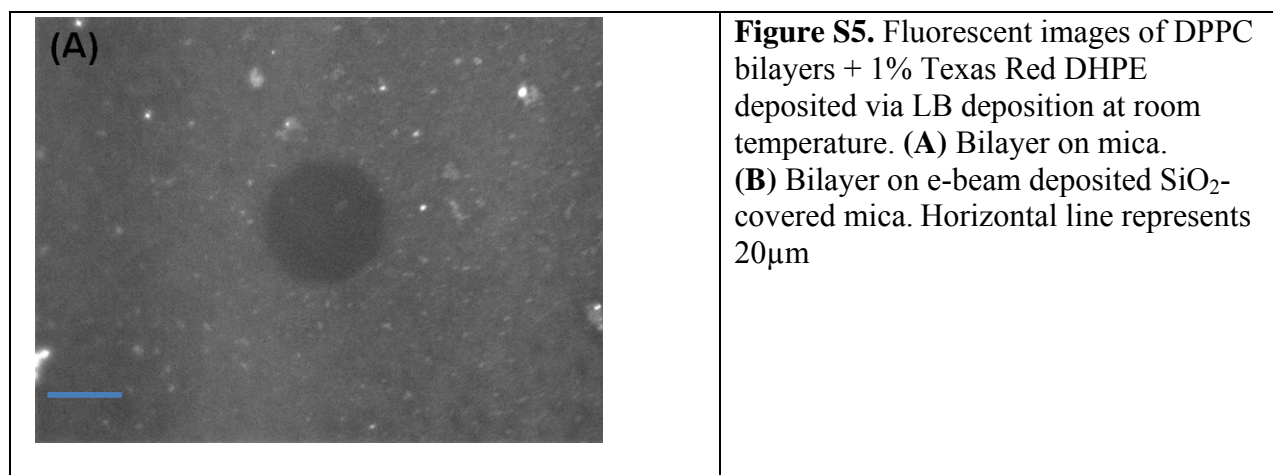
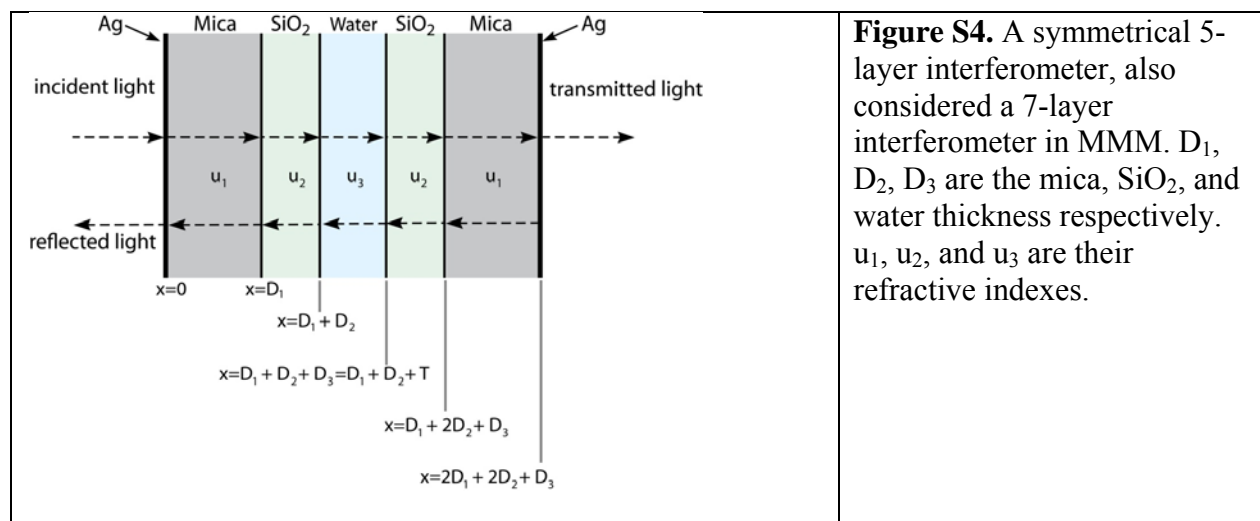
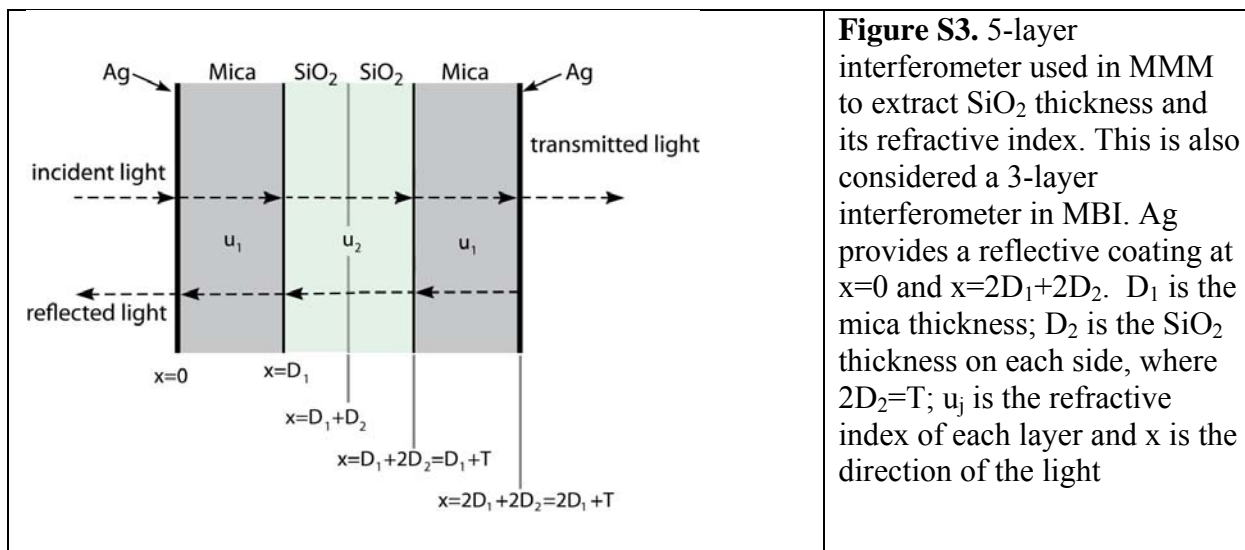
#### REFERENCES

1. Born, M. W., E., *Principles of Optics*. Pergamon Press: London, 1959.
2. Clarkson, M. T., Multi-beam interferometry with thin metal films and unsymmetrical systems. *Applied Physics* **1989**, 22, 475-482.

3. Heuberger, M. L., G.; Israelachvili, J., Topographic Information from Multiple Beam Interferometry in the Surface Force Apparatus. *Langmuir* **1997**, 13, 3839-3848.
4. Mangipudi, V. S., Analysis and Application of a 5-Layer Multiple Beam Interferometer in the Surface Forces Apparatus. *Colloid and Interface Science* **1995**, 175, 484-1995.
5. Israelachvili, J., Thin film studies using multiple beam interferometry. *J. Colloid Interface Science* **1973**, 44, 259.
6. Levins, J. M. V., T.K., Reduction of the Roughness of Silver Films by the Controlled Application of Surface Forces. *The Journal of Physical Chemistry* **1992**, 96, (25), 10405-10411.
7. Vigil, G. X., Z.; Steinberg, S.; Israelachvili, J., Interactions of Silica Surfaces. *Colloid and Interface Science* **1994**, 165, 367-385.
8. Kubitscheck, U. W., P. ; Peters, R. , Lateral diffusion measurement at high spatial resolution by scanning microphotolysis in a confocal microscope. *Biophys. J.* **1994**, 67 948–956.
9. Blonk, J. C. G. D., A.; Van Aalst, H.; Birmingham, J.J., Fluorescence photobleaching recovery in the confocal scanning light microscope. *J. Microscopy* **1992**, 169 363–374.
10. Axelrod, D.; Koppel, D. E.; Schlessinger, J.; Elson, E.; Webb, W. W., Mobility measurement by analysis of fluorescence photobleaching recovery kinetics. *Biophys. J.* **1976**, 16, 1055–1069.







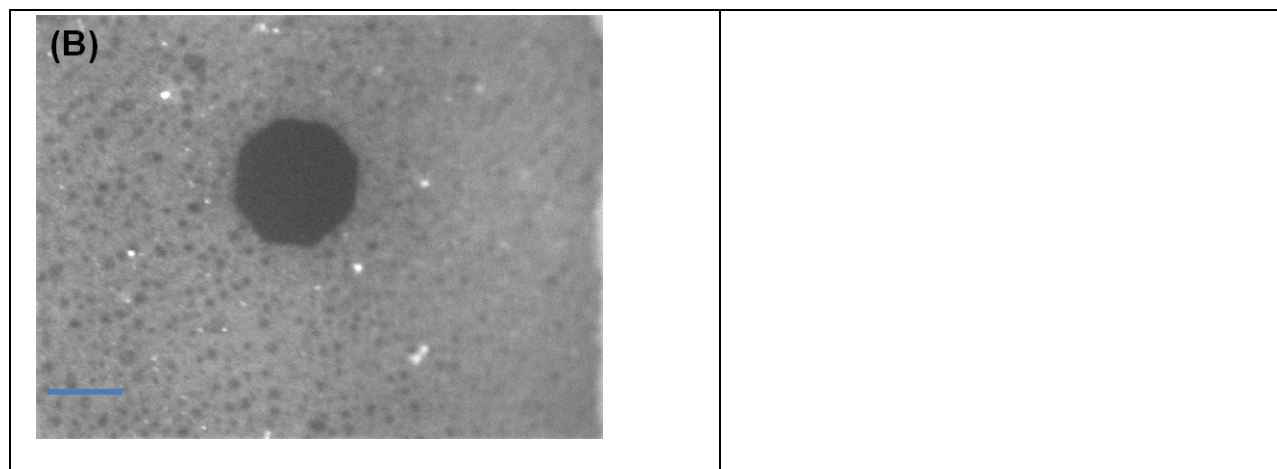


**Table S1.** SiO<sub>2</sub> thickness in air vs. water

	Thickness (Å)	RI	SSE
Quartz Crystal Reading	1000	--	--
In air using MMM	1028	1.46	0.0852
In water using MMM	1051	1.46	0.0042

**Table S2.** Comparing SiO<sub>2</sub> thickness using quartz crystal and MMM. The measurements are of SiO<sub>2</sub> surfaces in hard contact under water.

	SiO <sub>2</sub> Thickness from the Quartz Crystal Reading	SiO <sub>2</sub> Thickness in water using 3-Layer MMM (Å)	SiO <sub>2</sub> RI	SSE
Experiment A	1000	1051-1053	1.46	0.004+0.05
Experiment B	530	581-587	1.46-1.47	0.049+0.05
Experiment C	500	527-531	1.46-1.47	0.018+0.09

**Table S3.** Water thickness at different separations using MMM and BMI. The reference for MBI was SiO<sub>2</sub> contact in water.

Water Thickness (Å)				
MMM	3-Layer MBI	%Difference btw MMM and 3-Layer MBI	5-Layer MBI	%Difference btw MMM and 5-Layer MBI
0	0	----	0	----
196	171	12.8	190	3.4
402	363	9.7	403	0.3
836	783	6.3	862	3.0
1283	1232	4.0	1324	3.1
1672	1636	2.2	1712	2.3